Institute for
Shock Physics
Washington State University

"Graphite to Diamond Transformation under Shock Compression: Role of Orientational Order"

T. J. Volz and Y. M. Gupta

DOI: 10.1063/1.5108892

Published: June 2019

Journal of Applied Physics

Graphite to Diamond Transformation under Shock Compression: Role of Orientational Order

Travis J. Volz and Y. M. Gupta [a)]

Institute for Shock Physics and Department of Physics and Astronomy, Washington State University, Pullman, Washington 99164, USA

[a)] Electronic mail: ymgupta@wsu.edu

To gain insight into the role of orientational order on the shock-induced graphite to diamond phase transformation, three pyrolytic graphite types having different orientational orders were shock-compressed along the average *c*-axis to peak stresses between 35 and 69 GPa. The materials studied were ZYB-grade highly oriented pyrolytic graphite (HOPG), ZYH-grade HOPG, and as-deposited pyrolytic graphite (PG) having mosaic spreads of .8°±.2°, 3.5°±1.5°, and ~45°, respectively. Wave profiles, obtained using laser interferometry, show a multiple-wave structure with a distinct, rapid (<10 ns) rise to the high-pressure phase for each graphite type. Multiple-wave profiles, first observed in this study for the less ordered ZYH-grade HOPG and PG samples, show that somewhat poorly oriented pyrolytic graphites also undergo a well-defined phase transformation. Previously, rapid transformation was reported for ZYB-grade but not ZYH-grade HOPG. The measured wave profiles for both HOPG grades are very similar and both grades show a ~22 GPa transformation stress. In contrast, the PG wave profiles are quite different and show a ~46 GPa transformation stress. The continuum results (stress-density states) presented here cannot distinguish between the different high-pressure phases (hexagonal diamond (HD) or cubic diamond (CD)) reported in recent x-ray studies. Because ZYB-grade HOPG was recently shown to transform to HD and due to the similar peak states for both HOPG grades, it seems likely that ZYH-grade also transforms to HD. The very different shock responses of PG and HOPG suggest different transformation mechanisms for PG and HOPG, but the high-pressure PG phase remains unclear in the present work.

This manuscript was accepted by J. Appl. Phys. Click here to see the version of record.

I. INTRODUCTION

Cubic diamond (CD) was first recovered in the early 1960s by DeCarli and Jamieson from graphite samples shock compressed using high explosives.[1] Since then, the shock-induced graphite to diamond (G-D) phase transition has been an area of considerable scientific and technological interest. A wide range of studies involving Hugoniot measurements,[2–11] shock recovery experiments,[1,12–19] and atomistic modeling[20–24] have been carried out to better understand this phase transition. A good understanding of the shock-induced G-D phase transition and associated time scales is useful because it can provide insight into shock-induced phase transformation mechanisms[25] and because of its relevance to shock-synthesized diamonds[26,27] and meteorite impacts.[28–31]

Early Hugoniot experiments lacked the time-resolution required to determine the dynamics of this transition.[2–5] In the early 1990s, wave profile measurements on two types of shock-compressed HOPG samples were used to determine the transition timescales and to infer potential mechanisms associated with this transition.[7,8] The measured two-wave profiles for HOPG samples with the highest orientational order (ZYB-grade) showed a transformation stress of ~20 GPa and a sub-10 ns rise time to achieve the high-pressure phase. Due to the rapid transformation time, the authors concluded that the phase transition in the ZYB-grade was likely martensitic.[7,8] In contrast, the lesser oriented samples (ZYH-grade) did not show a two-wave structure, as evident from rounded and variable wave profiles. Analysis of the ZYH profiles suggested transition stresses ranging from 24 to 42 GPa.[7,8] Another study which examined two HOPG grades of greater orientational order than the ZYH-grade also provided evidence of a well-defined, two-wave structure for more oriented HOPG.[9]

To gain insight into the reported differences[7,8] between the shock response of ZYB and ZYH-grade HOPG, both grades were studied below the ~20 GPa transformation stress of the ZYB-grade.[10,11] Significant differences in the wave profiles[10] were observed between the two

HOPG grades below the phase transformation stress: the more oriented HOPG (ZYB) exhibited an elastic-inelastic wave structure while the less oriented HOPG (ZYH) exhibited a single wave. An increasing elastic wave amplitude with increasing peak stress led the authors to propose an elastic instability transformation mechanism for the ZYB-grade HOPG.[10]

The role of different starting materials on the shock-induced G-D transformation has been studied extensively since the first studies in the 1960s.[1,5–9,16] In addition to the lack of a distinct transformation stress indicated above for less oriented pyrolytic graphite, different high-pressure phases,[32,33] transformation stresses,[2,3,5–9] and transformation rates[7–9] have been reported for different types and qualities of starting materials. (Note, in this work 'pyrolytic graphite' is used to refer to either HOPG or PG, since 'PG' is used specifically to refer to as-deposited pyrolytic graphite.) These different materials include natural graphite, synthetic graphite, HOPG, and PG, which have different densities, microstructures, and crystallinities.[9,16,34] Despite the large range of starting materials examined, most graphite types subjected to high stresses under shock compression transform to a less compressible high-density phase.[2,4–6,8,9] Both cubic diamond[32] and hexagonal diamond[32,33] phases have been reported as the high-pressure phase in recent studies that utilized *in situ*, real-time, x-ray diffraction (XRD) measurements in different types of shock-compressed pyrolytic graphite.

Due to the large volume difference between the graphite and diamond phases, a two-wave structure is expected over certain stress ranges during the G-D transition:[8,25] the first wave takes the material to the transition stress and the second wave takes it to the peak state in the high-pressure phase. Two-wave structures have been observed for HOPG of sufficient orientational order, natural graphite, and synthetic graphite materials.[7,9] However, two-wave structures have not been observed for the less ordered ZYH-grade HOPG and PG. Although the transition is expected to occur between 34 and 56 GPa in PG,[5,6,32] time-resolved velocity measurements have not shown a two-wave structure.[6,32]

This manuscript was accepted by J. Appl. Phys. Click here to see the version of record.

While previous studies of the shock-induced G-D phase transformation have examined the effects of certain microstructures on the transformation,[9,16] there is uncertainty regarding the role of orientational order on the shock-induced G-D transformation. The present work was undertaken to answer the following questions: (1) Do pyrolytic graphite types with low orientational order exhibit a well-defined transformation stress? (2) Can wave profile measurements show rapid transformations in less oriented pyrolytic graphite samples? (3) Can wave profiles and calculated in-material states in pyrolytic graphites provide insight into possible G-D phase transformation mechanisms and the resulting high-pressure phases?

To address the above questions and to quantify the transition stresses and peak states, well-characterized plate impact experiments were conducted on three types of pyrolytic graphite up to 69 GPa. Using laser-interferometry, shock velocities and transmitted wave profiles were obtained in ZYB-grade HOPG, ZYH-grade HOPG, and as-deposited PG. The HOPG types are the same as studied in previous work.[7,8,10,11]

The remainder of this paper is organized as follows: the experimental methods are presented in Section II; the measured wave profiles are presented in Section III; the analysis methods and a discussion of the results are presented in Section IV. The main findings of this work are summarized in Section V. Additional details are summarized in the appendices.

II. EXPERIMENTAL METHODS

A. Sample characterization and preparation

All the graphite samples used in this study were obtained from Momentive Performance Materials (Strongsville, OH, USA). The measured average densities, determined using the Archimedean method, were: 2.263±.003 g/cm^3, 2.251±.002 g/cm^3, and 2.200±.003 g/cm^3 for ZYB-grade HOPG, ZYH-grade HOPG, and PG respectively. Densities and other relevant experimental parameters for the impact experiments are summarized in Table I. When possible,

sound speeds were measured using the pulse-echo technique[35] along the average *c*-axis at ambient conditions. For PG, the average longitudinal and shear sound speeds were 3.40 ± .03 km/s and .83±.02 km/s, respectively. Reliable sound speeds were not obtained in the HOPG samples due to the large acoustic attenuation, a problem noted in previous work.[10,36]

The mosaic spread in each graphite grade is a measure of the orientational order of the crystallites comprising the bulk material: the smaller the mosaic spread, the greater the orientational order of the sample. The mosaic spread is defined as full width at half maximum of the (002) orientation distribution function.[34] The mosaic spreads reported by the manufacturer for ZYB and ZYH-grade HOPG are .8°±.2° and 3.5°±1.5°, respectively. Although no mosaic spread values were reported by the manufacturer for the PG samples, the mosaic spread of a typical PG sample is expected to be around 45 degrees.[37] In addition to having a larger mosaic spread, the PG samples also have lower crystallinity than either HOPG type due to the increased disorder between adjacent basal plane layers in PG.[37,38]

The different graphite types examined in this study also have different surface features. For ZYB-grade HOPG, ZYH-grade HOPG, and PG, the surface height fluctuations, of as-received samples, are on the order of 0-3, 6-10, and 10-20 microns, respectively. The HOPG samples are comprised of many layers parallel to the face of each sample; in contrast, the PG samples are macroscopically more homogeneous. These differences resulted in different sample preparation methods for HOPG and PG. To achieve the desired HOPG sample thickness (reported in Table I), scotch tape was used to cleave layers off each sample face. Because the surface features of HOPG go through the entire sample, cleaving could not eliminate the features. In contrast, the as-received PG samples had approximately the desired thickness and were polished with optical polishing paper to reduce the surface roughness to around a micron.

B. Plate-impact experiments

This manuscript was accepted by J. Appl. Phys. Click here to see the version of record.

A schematic view of the experimental configuration is shown in Fig. 1. Using a two-stage light gas gun, an impactor was launched onto the target assembly consisting of the graphite sample sandwiched between a buffer and an optical window, bonded using 815 epoxy. Shock waves with peak stresses ranging between 35 and 69 GPa were propagated into the graphite samples along the average *c*-axis. For shock waves below 52 GPa, 1050 aluminum was used for impactors, while higher stress experiments used C101 copper impactors. In each experiment, the impactor and buffer were made of the same material to prevent wave reflection from the impactor/buffer interface. The lateral dimensions of all components were chosen to ensure that the data would be obtained during uniaxial strain compression (before edge release waves or longitudinal release waves reach the probed region).

To measure wave profiles at the sample/window interface using a VISAR,[39,40] a mirror was vapor-deposited on the lithium fluoride window before bonding it to the sample. Use of dual velocity-per-fringe for the center VISAR probe enabled unambiguous particle velocity measurements at the sample/window interface. The three radial VISAR probes, focused on the back of the polished buffer at 120° intervals, allowed a determination of the shock arrival time at the sample/buffer interface. The VISAR probes provided shock transit times through the sample and wave profiles at the sample/window interface. As discussed later, these measurements were used to obtain in-material, stress-volume states.

III. RESULTS

A total of 16 impact experiments were conducted in this study and the relevant experimental parameters are summarized in Table I. Representative particle velocity profiles measured at the sample/window interface for ZYB-grade HOPG, ZYH-grade HOPG, and PG are shown in Figs. 2-4, respectively, and discussed below. Time t=0 in each plot corresponds to the shock wave arrival at the buffer/sample interface, and the wave profiles shown are for times when the sample is in a state of uniaxial strain.

This manuscript was accepted by J. Appl. Phys. Click here to see the version of record.

Measured shock and particle velocities, and the resulting in-material, longitudinal stress-volume states are listed in Tables II and III. The analytic procedure used to obtain the in-material states shown in the two tables is described in Section IV.

A. ZYB-grade HOPG

In experiment 1, at the lowest peak stress, the measured wave profile consisted of a 3-wave structure: an elastic jump, a gradually rising second wave corresponding to the phase transition onset, and a sharp third wave resulting in the peak state in the high-pressure phase. The distinctions between the elastic jump, the phase change onset, and the sharp third wave become less clear with increasing peak stress – as seen in experiments 2 and 3 – due to the increasing wave velocity of the third wave. In experiment 4, the multiple wave structure is not observed because the high pressure phase can be attained by a single wave (overdriven case).

B. ZYH-grade HOPG

Overall, the wave profiles for the ZYH-grade shown in Fig. 3 are fairly similar to the ZYB profiles. The main differences between the profiles in Figs. 2 and 3 are in the structure between the first jump and the phase transition onset, and in the lack of a clear three wave structure even at the lowest peak stress in Fig. 3. We note these differences between Figs. 2 and 3 for completeness, but are not able to link these differences to specific features regarding the compressive states for the two HOPG grades.

An important aspect of the wave profiles shown in Fig. 3 is the significant difference between the present ZYH profiles and the ZYH profile reported by Erskine and Nellis.[7] Unlike the multiple waves clearly observed in our experiments, only a rounded single wave to a peak state with velocity fluctuations was reported previously.[7] The ZYH-grade HOPG samples in this study were from the same source as earlier experiments[7,8] and are expected to have similar material characteristics. The present and previous ZYH samples had similar densities of 2.251

This manuscript was accepted by J. Appl. Phys. Click here to see the version of record.

and 2.262 g/cm^3,[7] respectively, but the physical appearance of the previous ZYH samples was reportedly different. The earlier samples had a "dull 'pencil-lead' appearance," possibly similar to the PG samples in this study, but unlike the metallic luster of our HOPG samples. We are unable to explain why only a rounded wave was observed in the earlier work on ZYH-grade HOPG, since rapidly rising, well-defined shocks were observed in our experiments for both the ZYH-grade HOPG and the precursor PG material, discussed next.

C. PG

Experiment 9, showing a clear single wave, resulted in a peak stress of 39 GPa in the graphite phase — well above the ~22 GPa phase transition stress observed for both HOPG grades. At higher peak stresses (experiments 10-15), clear two-wave structures were observed. To the best of our knowledge, the two-wave structures observed for PG in this work are the first such observations. Finally, in experiment 16 (peak stress 69 GPa), a single wave corresponding to an overdriven transition was observed. The measured wave profiles show that the PG stays in the graphite phase up to 46 GPa, more than twice the phase transformation stress observed in the HOPG grades.

The similarities in wave profiles and peak stresses achieved in comparable experiments demonstrate good experimental reproducibility. Experiments 5 and 6 showed good reproducibility between ZYH-grade HOPG experiments, though slightly different sample thicknesses gave profiles displaced in time. The results in Table III for experiments 11 and 12 show good reproducibility between PG experiments, though the large difference between these two experiments and a similar experiment 10 are not understood.

As discussed in Appendix A, a systematic experimental error was observed in the shock velocity measurements in experiments 13 and 14. The cause of this error was identified and the

This manuscript was accepted by J. Appl. Phys. Click here to see the version of record.

experimental design was modified for the high stress experiments. The results shown in Table III for experiments 13 and 14 were obtained by using the correct shock velocity measurements.

IV. ANALYSIS AND DISCUSSION

A. Determination of end states

To determine the transition stresses and peak states, the wave profiles were analyzed using impedance matching techniques and the Rankine-Hugoniot jump conditions. These methods are well established,[41,42] but are briefly summarized in Appendix B for completeness.

In the analysis used here, the wave profiles are approximated as 1, 2, or 3 step shocks and impedance matching is carried out in the $P_x - u_p$ plane accounting for wave reflections from the LiF window. The reflected Hugoniot approximation (a reasonable assumption)[43] is used for the buffer to determine the peak $P_x - u_p$ state in each case. The Rankine-Hugoniot jump conditions are then used to determine the in-material longitudinal stress - volume states achieved after each subsequent shock. The results of this analysis are reported in Tables II and III and longitudinal stress-volume states are plotted in Figs. 5 and 6.

The analytical procedure used here is similar to that used by Erskine and Nellis[8] and provides results that are quite consistent with a more rigorous approach using a wave propagation code.[44]

B. HOPG

The two HOPG grades demonstrated very comparable in-material stress-volume states over the full range of stresses examined in this work as shown in Fig. 5 by the overlap of the calculated states. At the transformation, the ZYB and ZYH-grades exhibit very comparable stress-volume states, (21.9±0.4 GPa, .3606 cm^3/g) and (21.5±0.7 GPa, .3610 cm^3/g),

respectively. The transformation states also show good agreement with an extrapolation of HOPG Hugoniot data from below the transformation stress[10] (shown in Fig. 5 as open triangles). The in-material transition state from experiment 3 was not included in the above values because the transformation stress was much higher than any other observed ZYB onset in previous work[8] and the present study. Above the transformation stress, the peak states are again consistent for both HOPG grades. These states are also consistent with the hexagonal diamond (HD) response shown as the gray band[33] in Fig. 5 and discussed next.

Based on *in situ* x-ray measurements, it was recently reported that ZYB-grade HOPG shock-compressed along the average *c*-axis transforms to HD (with the $[10\bar{1}0]$ HD direction along the loading direction).[33] Because of the unavailability of HD as a bulk material at ambient conditions, determination of the HD elastic Hugoniot (in contrast to the CD elastic Hugoniot) requires a theoretical approach[33] resulting in the gray band shown in Fig. 5. The width of the gray band reflects the range of the XRD-determined HD densities, as discussed in Ref. 33. A previous study[44] utilizing experimentally determined CD shock response[45] showed that the peak stress-volume states in the high pressure phase of the shock-compressed ZYB-grade HOPG (up to 58 GPa) correspond to the CD elastic Hugoniot. The main point to be emphasized is that the high-pressure stress-volume states, though determined accurately from the wave profiles, cannot distinguish between HD and CD phases. XRD measurements[33] were required to establish the high pressure phase of shock-compressed HOPG.

C. PG

In contrast to the comparable shock response of both HOPG grades, the in-material stress-volume states are quite different between PG and HOPG at the respective transformation stresses. This can be readily seen by comparing the in-material states plotted in Figs. 5 and 6. As shown in Fig. 6, the PG states — prior to the transformation — are closely bunched together

and have an average stress-volume value: 46 GPa, .323 cm^3/g. The in-material state from experiment 10 was not included in the average because it is inconsistent with all our other data. Our results clearly demonstrate that the transformation stress in PG is more than twice the transformation stress of either HOPG grade (46 GPa vs 22 GPa). Additionally, the calculated specific volumes for the PG samples at the transition are significantly lower than for the HOPG samples (~.323 cm^3/g vs ~.360 cm^3/g); PG is more compressed prior to the transformation. Overall, the in-material states and the transformation stress determined here are generally consistent with the previously reported PG Hugoniot data.[3,5,6,46]

The clear two-wave structures observed in the PG experiments provide information not obtained in earlier experiments — in-material states both before and after the transition were determined. Previous studies provided only a single state per experiment since no two-wave structures were observed.[3,5,6,46] At ~50 GPa, just above the transformation, the peak states (experiments 11 and 12) have a slightly larger volume than expected for either high-pressure phase. This may suggest either a mixed phase or that the transformation is not yet complete. At higher stresses, the PG peak states are quite consistent with either the CD or the HD phase. A recent *in situ*, real-time XRD study of laser-shocked PG samples reported CD as the high-pressure phase near 50 GPa.[32] Because different PG suppliers were used in the present work and in the XRD study[32] and because the experimental methods in the present work (plate impact resulting in longer durations) and in the XRD study (laser-shock resulting in shorter durations) were very different, it is difficult to conclude from the present work that the stress-volume states shown in Fig. 6 correspond to the CD phase. Hence, both phases are shown in Fig. 6 for completeness.

D. Discussion

This manuscript was accepted by J. Appl. Phys. Click here to see the version of record.

Multiple-wave profiles, first reported here for ZYH-grade HOPG and PG, demonstrate that well-defined phase transition stresses exist for pyrolytic graphites with mosaic spreads of 3.5°±1.5° and larger. For ZYH-grade HOPG, the consistent ~21.5 GPa transformation stress observed in this work is in marked contrast to the large range of transition stresses (24-42 GPa) reported previously for ZYH-grade HOPG.[7,8] For PG, the ~46 GPa transformation stress is near the range of PG transformation stresses suggested in previous studies.[5,6,32] In addition to determining the transformation stresses for less oriented pyrolytic graphite samples, the wave profiles reported here demonstrate the rapidity of the observed transformations.

The wave profiles show $\lesssim$ 5 ns rise times to the peak states in the high-pressure phase for each HOPG experiment as well as for PG experiments above 60 GPa peak stress. The calculated stress-volume states in each of the aforementioned experiments are consistent with the diamond phases. This suggests that the phase transformation to the high-pressure phase is complete within the rise time of the final wave since the calculated states characterize the peak states attained. In PG, rapid transformations were previously suggested based on the XRD measurements showing CD formation on nanosecond time scales[32] and conductivity measurements showing a rapid change to an insulating high-pressure phase.[47] Our wave profile measurements directly show this rapid transformation wave and provide support for previous inferences of a rapid transformation in PG. The rapid transformations observed for each pyrolytic graphite type suggest that decreased crystallite alignment and other material differences do not increase the transformation times for sufficient input stresses.

Although, the main focus of the present paper is on wave profile measurements and calculated stress-volume states, some insight can be gained regarding the transformation mechanisms and the resulting high-pressure phases.

The very similar shock responses of ZYB and ZYH-grade HOPG, suggest that the high-pressure phases and transformation mechanisms for both grades may be similar. Thus, it is likely that the ZYH-grade also transforms to HD and that the orientation relations are the same as reported for the ZYB-grade. Although the formation of HD with the orientation observed in shock experiments[33] has not been predicted in shock-wave atomistic simulations,[21,24] epitaxial arguments[48] and non-shock simulations[22,23] have proposed the observed orientation relation. Thus, the concerted shifting and buckling mechanism proposed[22,23,48] may describe the atomistic pathways in our work for both HOPG grades. A similar transformation mechanism for both HOPG grades would rule out the previously proposed elastic instability transformation mechanism, suggested only for the ZYB-grade HOPG.[10] The observation of a three-wave structure in ZYB-grade HOPG experiments 1 and 2 also casts doubt on the elastic instability mechanism since the phase change onset wave occurs after the elastic wave.

At the transformation, PG has a much higher stress and a smaller specific volume than either HOPG grade. This suggests that the PG response is quite different from HOPG prior to the transformation. Above the transformation, the stress-volume states are also different for HOPG and PG: the HOPG peak states are consistent with HD by ~35 GPa, whereas the PG peak states are not consistent with a diamond phase until near 60 GPa. These differences suggest that the transformation mechanisms are likely different for HOPG and PG. A different atomistic mechanism would also be required to explain the results of the recent XRD study of shock-compressed PG, which reported the formation of CD, not HD, as the high-pressure phase near 50 GPa.[32]

Although the continuum results presented here have provided accurate stress-volume response for the three types of pyrolytic graphite examined, these results lack crystallographic and microstructural information regarding the high-pressure phase. Above 55 GPa, the in-material states determined in this work are comparable for all three graphite types. However,

This manuscript was accepted by J. Appl. Phys. Click here to see the version of record.

recent real-time XRD results reported that, near 50 GPa, ZYB-grade HOPG transforms to HD[33] whereas PG transforms to CD.[32] Because of differences in the starting material (HOPG vs. PG) and in the loading conditions, it is difficult to provide an obvious explanation for this difference. Similar to the HOPG samples in Ref. 33, XRD measurements on PG samples using plate impact experiments will be required to address this issue.

V. SUMMARY

To examine the role of graphite orientational order on the shock-induced G-D phase transition, plane shock wave experiments were carried out on three pyrolytic graphite types with different orientational orders: ZYB-grade HOPG, ZYH-grade HOPG, and PG. Wave profiles and shock velocities were obtained for samples shock-compressed along the average *c*-axis to peak stresses ranging from 35 to 69 GPa. These data were used to obtain transformation times, precisely determine in-material states, and to gain insight into potential transformation mechanisms. The main findings from this work are summarized below:

1) Multiple wave profiles, characteristic of a rapid phase transformation, were observed for each pyrolytic graphite type, regardless of orientational order. For ZYH-grade HOPG and PG, these are the first such observations.
2) Analysis of the measured shock velocities and wave profiles have provided accurate longitudinal stress-volume states for each of the three graphite types.
3) Transformation stresses of ~22 GPa were determined for both HOPG grades, whereas the transformation stress for PG was ~46 GPa.
4) The peak states for both HOPG grades are consistent with HD, the recently reported phase of ZYB-grade HOPG shocked to 50 GPa.[33]
5) The peak states for the PG samples shock-compressed to 50 GPa are less dense than those expected for a diamond phase. However, at higher stresses, the peak states are compatible with either the CD or the HD phase.

The present results show that pyrolytic graphite types, even with larger mosaic spreads, undergo rapid, well-defined phase transformations. Very similar shock responses for both HOPG grades suggest similar transformation mechanisms and, likely, similar high-pressure phases. In contrast, for PG, which has a much larger mosaic spread, a different transformation mechanism seems probable based on the higher transition stress and different in-material states. To accurately determine the structures of the high-pressure phases of the ZYH-grade HOPG and PG samples examined in this work and to gain insight into the structural response below the transition, *in situ* real-time XRD measurements during shock-compression are needed.

ACKNOWLEDGEMENTS

Nate Arganbright, Thomas Eldredge, Kurt Zimmerman and Yoshi Toyoda are sincerely thanked for their assistance with these experiments. Discussions with Drs. Surinder Sharma, Stefan Turneaure, and Michael Winey regarding the G-D transformation are gratefully acknowledged. This work was supported by DOE NNSA Cooperative Agreement DE-NA0002007.

APPENDIX A: WAVE SPEED ERROR AND CORRECTION

For a constant or an increasing phase transformation stress in a material, the measured first shock speed should remain constant or increase slightly. Since the calculated first wave speeds in experiments 13 and 14 were much slower than even the lower stress experiments 11

and 12, it pointed to a systematic error in our wave transit time measurements, because the PG sample thicknesses were precisely measured to within a micron.

The shock arrival at the front of the sample was determined from the shock arrival times at the radial VISAR probes at the buffer rear surface and the assumption of a planar impact. Using separate experiments designed to directly measure the impact times across the face of the ~3mm thick C101 Cu impactor, it was determined that impact at the center occurred more than 25 ns after impact at the radial probe locations; the impactor was bowing inwards and did not satisfy the assumption of a planar impact.

Several different impactor configurations were examined and tested. It was determined that by using a 1 mm thick Cu impactor, impact at the center occurred within 1 ns (measurement resolution) of a planar impact at the radial probe locations. Subsequently, this configuration was used for experiment 15 and the shock velocity obtained for experiment 15 was then used to analyze experiments 13 and 14.

APPENDIX B: DETERMINATION OF END STATES

The in-material states corresponding to the wave profiles in Figs. 2-4 were determined using the Rankine-Hugoniot jump conditions and impedance matching[41,42] along with the measured shock and particle velocities. For experiments 4, 8, 9, and 16, where single waves were observed, the shock velocities and published Hugoniot data for the buffer materials (1050 Al[49] or C101 Cu[50]) were used to directly determine the shocked in-material states.

For the experiments where two or three-wave profiles were observed, impedance matching in the $P_x - u_p$ plane was necessary to determine the in-material states. As shown in Fig. 7, the first and second shocks take the graphite from state 0 to state 1 and from state 1 to state 2, respectively. When the first wave encounters the LiF window, a small shock reflects back into the graphite resulting in the observed state 1', which can be determined using the known [100] LiF Hugoniot.[50] To determine state 1, we assume the magnitude of the slope of

lines $\overline{11'}$ and $\overline{12}$, in Fig. 8, are equal. This assumption introduces little error since the impedances of the ambient graphite and LiF are very similar. This assumption fixes both states 1 and 2 using only the observed shock and particle velocities and the known Hugoniots.[49,50] A similar equal slope treatment is used for the first two shocks in the three wave case, since in the three wave case, both states 1 and 2 lie close to the LiF Hugoniot.

References

[1] P. S. DeCarli and J. C. Jamieson, Science **133**, 1821 (1961).

[2] B. J. Alder and R.H. Christian, Phys. Rev. Lett. **7**, 367 (1961).

[3] N. L. Coleburn, J. Chem. Phys. **40**, 71 (1964).

[4] M. N. Pavlovskii and V. P. Drakin, JETP Lett. **4**, 169 (1966).

[5] R. G. McQueen and S. P. Marsh, in *Behavior of Dense Media under High Dynamic Pressure* (Gordon and Breach, New York,1968), p. 207.

[6] W. H. Gust, Phys. Rev. B **22**, 4744 (1980).

[7] D. J. Erskine and W. J. Nellis, Nature **349**, 317 (1991).

[8] D. J. Erskine and W. J. Nellis, J. Appl. Phys. **71**, 4882 (1992).

[9] G. I. Kanel, G. S. Bezruchko, A. S. Savinykh, S. V. Razorenov, V. V. Milyavskii, and K. V. Khishchenko, High Temp. **48**, 806 (2010).

[10] M. Lucas, J. M. Winey, and Y. M. Gupta, J. Appl. Phys. **114**, 093515 (2013).

[11] M. Lucas, J. M. Winey, and Y. M. Gupta, J. Appl. Phys. **118**, 245903 (2015).

[12] L. F. Trueb, J. Appl. Phys. **39**, 4707 (1968).

[13] D. G. Morris, J. Appl. Phys. **51**, 2059 (1980).

[14] H. Hirai and K. Kondo, Science **253**, 772 (1991).

[15] G. Burkhard, K. Dan, Y. Tanabe, A. B. Sawaoka, and K. Yamada, Jpn. J. Appl. Phys. **33**, 876 (1994).

[16] H. Hirai, S. Kukino, and K. Kondo, J. Appl. Phys. **78**, 3052 (1995).

[17] A. Z. Zhuk, T. I. Borodina, V. E. Fortov, A. A. Lash, and G. E. Val'iano, High Press. Res. **15**, 245 (1997).

[18] K. Yamada and Y. Tanabe, Carbon N. Y. **40**, 261 (2002).

[19] T. Sano, K. Takahashi, O. Sakata, M. Okoshi, N. Inoue, K.F. Kobayashi, and A. Hirose, J. Phys. Conf. Ser. **165**, 012019 (2009).

[20] S. Scandolo, M. Bernasconi, G. L. Chiarotti, P. Focher, and E. Tosatti, Phys. Rev. Lett. **74**, 4015 (1995).

[21] C. J. Mundy, A. Curioni, N. Goldman, I.-F. W. Kuo, E. J. Reed, L. E. Fried, and M. Ianuzzi, J. Chem. Phys. **128**, 184701 (2008).

[22] R. Z. Khaliullin, H. Eshet, T.D. Kühne, J. Behler, and M. Parrinello, Nat. Mater. **10**, 693 (2011).

[23] P. Xiao and G. Henkelman, J. Chem. Phys. **137**, 101101 (2012).

[24] N. Pineau, J. Phys. Chem. C **117**, 12778 (2013).

[25] G. E. Duvall and R. A. Graham, Rev. Mod. Phys. **49**, 523 (1977).

[26] P. S. DeCarli, US Patent No. 3,238,019 (1966).

[27] G. R. Cowan, B. W. Dunnington, and A. H. Holtzman, US Patent No. 3,401,019 (1968).

[28] M. E. Lipschutz, Science **143**, 1431 (1964).

[29] R. E. Hanneman, H. M. Strong, and F. P. Bundy, Science **155**, 995 (1967).

[30] R. S. Clarke Jr, D. E. Appleman, and D. R. Ross, Nature **291**, 396 (1981).

[31] Y. Nakamuta and S. Toh, Am. Mineral. **98**, 574 (2013).

[32] D. Kraus, A. Ravasio, M. Gauthier, D.O. Gericke, J. Vorberger, S. Frydrych, J. Helfrich, L.B. Fletcher, G. Schaumann, B. Nagler, B. Barbrel, B. Bachmann, E.J. Gamboa, S. Göde, E. Granados, G. Gregori, H.J. Lee, P. Neumayer, W. Schumaker, T. Döppner, R.W. Falcone, S.H. Glenzer, and M. Roth, Nat. Commun. **7**, 10970 (2016).

[33] S. J. Turneaure, S. M. Sharma, T. J. Volz, J. M. Winey, and Y. M. Gupta, Sci. Adv. **3**, eaao3561 (2017).

[34] A. W. Moore, in *Chem. Phys. Carbon*, edited by P. L. Walker Jr and P. A. Thrower (Dekker, New York, 1973), Vol. 11, p. 69.

[35] H. J. McSkimin and P. Andreatch, J. Acoust. Soc. Am. **34**, 609 (1962).

[36] J. F. Green, P. Bolsaitis, and I. L. Spain, J. Phys. Chem. Solids **34**, 1927 (1973).

[37] O. J. Guentert and S. Cvikevich, in *Proc. Fifth Carbon Conf., Pennsylvania State University, 1961*, (Pergamon Press, New York, 1962), p. 473.

[38] W. H. Smith and D. H. Leeds, in *Mod. Mater.*, edited by B.W. Gonser (Academic Press, Inc., New York, 1970), Vol. 7, p. 139.

[39] L. M. Barker and R. E. Hollenbach, J. Appl. Phys. **43**, 4669 (1972).

[40] W. F. Hemsing, Rev. Sci. Instrum. **50**, 73 (1979).

[41] R. G. McQueen, S. P. Marsh, and J. N. Fritz, J. Geophys. Res. **72**, 4999 (1967).

[42] S. J. Turneaure, J. M. Winey, and Y. M. Gupta, J. Appl. Phys. **100**, 065322 (2006).

[43] W. J. Nellis, A. C. Mitchell, and D. A. Young, J. Appl. Phys. **93**, 304 (2003).

[44] J. M. Winey and Y. M. Gupta, Phys. Rev. B **87**, 174104 (2013).

[45] J. M. Lang Jr. and Y. M. Gupta, Phys. Rev. Lett. **106**, 125502 (2011).

[46] D. G. Doran, J. Appl. Phys. **34**, 844 (1963).

[47] A. C. Mitchell, J. W. Shaner, and R. N. Keeler, Physica **139**, 386 (1986).

[48] K. Lonsdale, Am. Mineral. **56**, 333 (1971).

[49] D. Choudhuri and Y.M. Gupta, AIP Conf. Proc. **1426**, 755 (2012).

[50] P. A. Rigg, M. D. Knudson, R. J. Scharff, and R. S. Hixson, J. Appl. Phys. **116**, 033515 (2014).

Figures

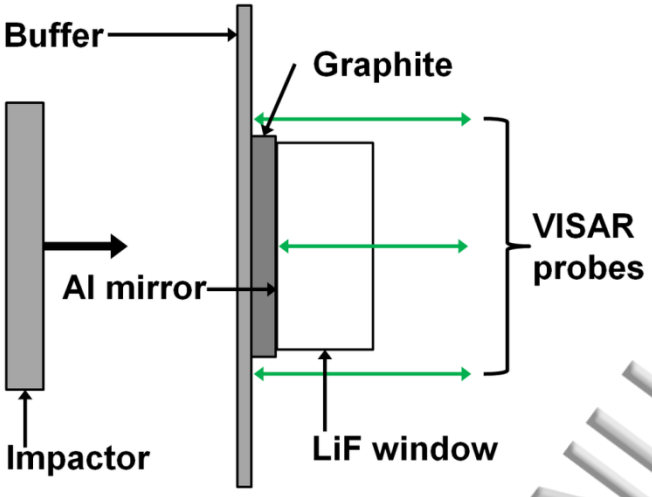

FIG. 1. Experimental configuration used for transmitted wave profile measurements in plate impact experiments.

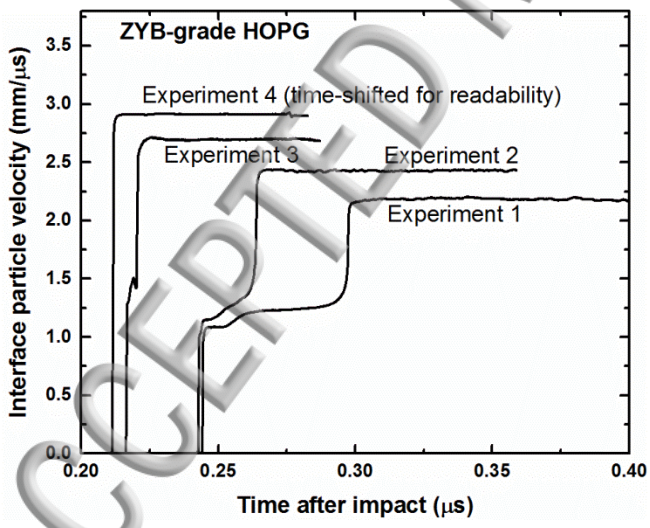

FIG. 2. Wave profiles obtained from ZYB-grade HOPG at the HOPG/LiF window interface. Time t=0 corresponds to the shock arrival at the buffer/sample interface. Experiment 1 wave profile was reported previously in Ref. 33.

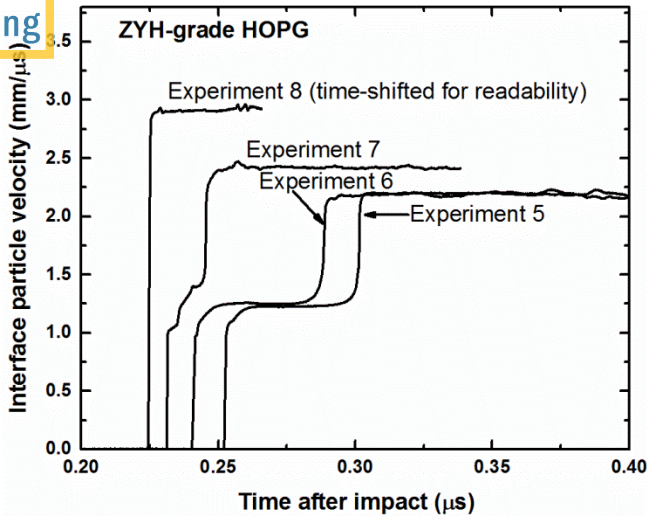

FIG. 3. Wave profiles obtained from ZYH-grade HOPG at the HOPG/LiF window interface. Time t=0 corresponds to the shock arrival at the buffer/sample interface.

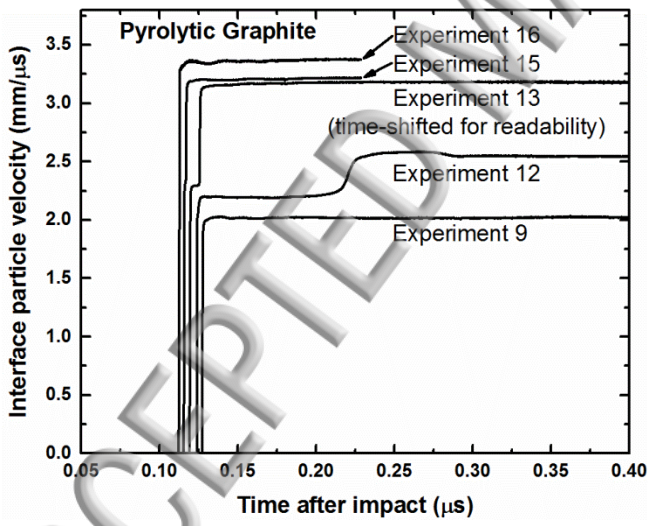

FIG. 4. Wave profiles obtained from PG at the PG/LiF window interface. Time t=0 corresponds to the shock arrival at the buffer/sample interface. Wave profiles for PG experiments 10, 11, and 14 were consistent with profiles shown here and were omitted for viewing clarity.

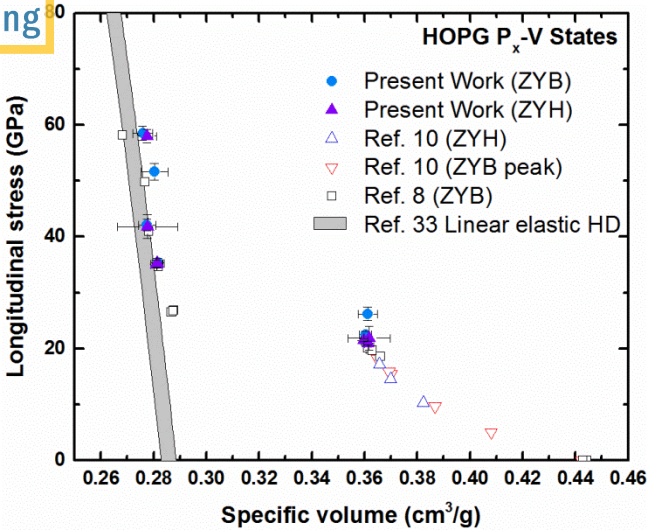

FIG. 5. Longitudinal stress vs specific volume for both grades of HOPG. The linear elastic hexagonal diamond (HD) curve is plotted for comparison, because recent XRD experiments showed HD to be the high-pressure structure[33] for the ZYB-grade HOPG.

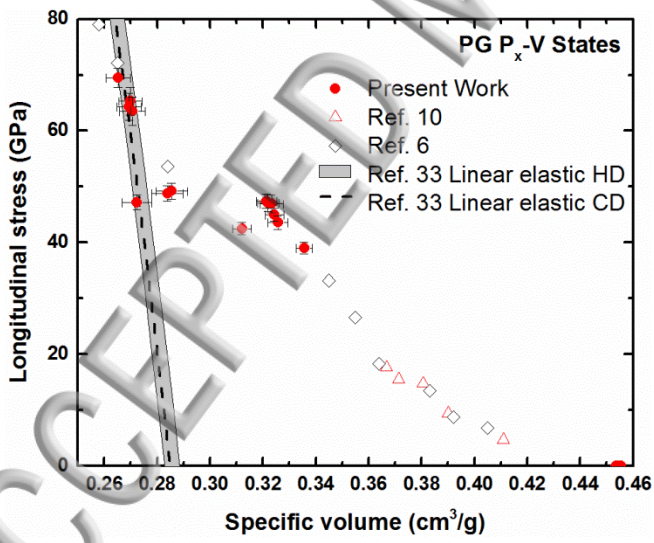

FIG. 6. Longitudinal stress vs specific volume for the PG experiments. The linear elastic HD and CD curves are plotted for comparison, because the high-pressure structure of PG in the present work is unknown.

This manuscript was accepted by J. Appl. Phys. Click here to see the version of record.

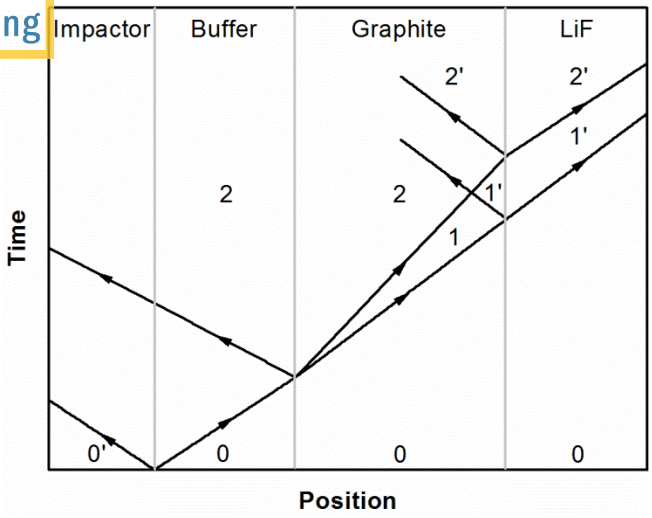

FIG. 7. Schematic diagram of wave propagation and in-material states achieved during a wave transmission experiment resulting in a two-wave profile.

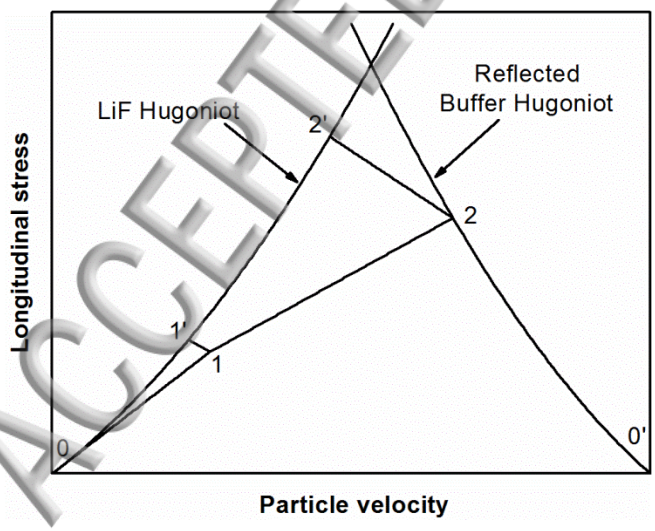

FIG. 8. $P_x - u_p$ diagram illustrating states achieved at the sample window interface (1' and 2') and in the graphite (1 and 2).

Tables

TABLE I. Experimental parameters for plate impact experiments.

Experiment number	Sample	Sample density (g/cm^3)	Sample thickness (mm)	Impactor/buffer material	Impact velocity (mm/μs)
1	ZYB	2.26	1.754	1050 Al	4.090
2	ZYB	2.26	1.788	1050 Al	4.592
3	ZYB	2.26	1.721	1050 Al	5.171
4	ZYB	2.26	1.013	C101 Cu	4.270
5	ZYH	2.25	1.771	1050 Al	4.091
6	ZYH	2.25	1.703	1050 Al	4.107
7	ZYH	2.25	1.675	1050 Al	4.590
8	ZYH	2.25	1.085	C101 Cu	4.258
9	PG	2.20	1.044	1050 Al	4.013
10	PG	2.20	1.111	1050 Al	5.024
11	PG	2.20	1.060	1050 Al	5.026
12	PG	2.20	1.047	1050 Al	5.035
13	PG	2.20	0.895	C101 Cu	4.649
14	PG	2.20	1.010	C101 Cu	4.683
15	PG	2.20	0.991	C101 Cu	4.719
16	PG	2.20	0.979	C101 Cu	4.946

TABLE II. Summary of HOPG results.

Exp. number	Sample	Elastic				Pre-transformed				Transformed			
		Shock velocity (mm/μs	Particle velocity [a] (mm/μs)	Long. stress (GPa)	Specific volume (cm^3/g)	Shock velocity [b] (mm/μs)	Particle velocity [a] (mm/μs)	Long. stress (GPa)	Specific volume (cm^3/g)	Shock velocity [b] (mm/μs)	Particle velocity [a] (mm/μs)	Long. stress (GPa)	Specific volume (cm^3/g)
1 [c]	ZYB	7.19±.09	1.084±.005	18.4±.3	.3729±.0013	6.83±.08	1.235±.006	21.3±.4	.3607±.0017	5.90±.06	2.185±.011	35.3±.8	.2817±.0023
2	ZYB	7.39±.07	1.147±.006	19.8±.3	.3707±.0009	7.11±.07	1.283±.035	22.5±.6	.3605±.0023	6.79±.06	2.428±.012	42.1±1.0	.2775±.0033
3 [c]	ZYB		No elastic wave observed			7.98±.11	1.419±.071	26.2±1.2	.3613±.0036	7.83±.11	2.696±.013	51.6±1.5	.2804±.0051
4	ZYB		No elastic wave observed				Only one wave observed			8.26±.21	2.910±.015	58.3±1.6	.2751±.0045
5	ZYH		No elastic wave observed			7.06±.08	1.226±.006	21.0±.3	.3613±.0013	5.89±.06	2.191±.011	35.1±.7	.2811±.0021
6	ZYH		No elastic wave observed			7.08±.09	1.249±.006	21.5±.3	.3598±.0013	5.91±.06	2.197±.011	35.3±.8	.2814±.0021
7	ZYH		No elastic wave observed			7.25±.08	1.265±.148	21.9±2.1	.3618±.0080	6.83±.07	2.419±.012	41.8±2.1	.2777±.0115
8	ZYH		No elastic wave observed				Only one wave observed			8.28±.20	2.906±.015	58.0±1.4	.2775±.0041

[a] Particle velocities reported here are at the LiF/sample interface
[b] Shock velocities reported in the Table are the Lagrangian shock velocities.
[c] Stress-volume states reported previously in Ref. 33.

TABLE III. Summary of PG results.

Experiment number	Pre-transformed				Transformed			
	Shock velocity (mm/μs)	Particle velocity [a] (mm/μs)	Longitudinal stress (GPa)	Specific volume (cm^3/g)	Shock velocity [b] (mm/μs)	Particle velocity [a] (mm/μs)	Longitudinal stress (GPa)	Specific volume (cm^3/g)
9	8.21±.19	2.021±.010	39.0±1.0	.3357±.0030		Only one wave observed		
10	7.86±.16	2.143±.011	42.5±1.1	.3121±.0036	4.93±.06	2.584±.013	47.2±1.3	.2724±.0056
11	8.36±.20	2.148±.011	43.6±1.2	.3257±.0037	5.07±.07	2.574±.013	48.8±1.4	.2839±.0059
12	8.44±.18	2.194±.011	45.0±1.2	.3244±.0035	4.75±.06	2.577±.013	49.2±1.4	.2855±.0060
13	8.58±.25 [c]	2.293±.011	46.9±1.6	.3233±.0044	8.08±.22	3.179±.016	63.5±2.5	.2707±.0049
14	8.58±.23 [c]	2.302±.012	47.1±1.5	.3220±.0041	8.21±.21	3.201±.016	64.3±2.4	.2695±.0046
15	8.58±.20	2.313±.028	47.4±1.3	.3214±.0038	8.46±.19	3.208±.016	65.3±2.5	.2699±.0043
16		Only one wave observed			8.71±.21	3.365±.017	69.5±1.7	.2653±.0047

[a] Particle velocities reported here are at the LiF/sample interface
[b] Shock velocities reported in the table are the Lagrangian shock velocities.
[c] Because of impactor bowing in experiments 13 and 14, the shock velocities shown for these two experiments is the same as experiment 15, which used a different impactor design to minimize bowing (see Appendix A).

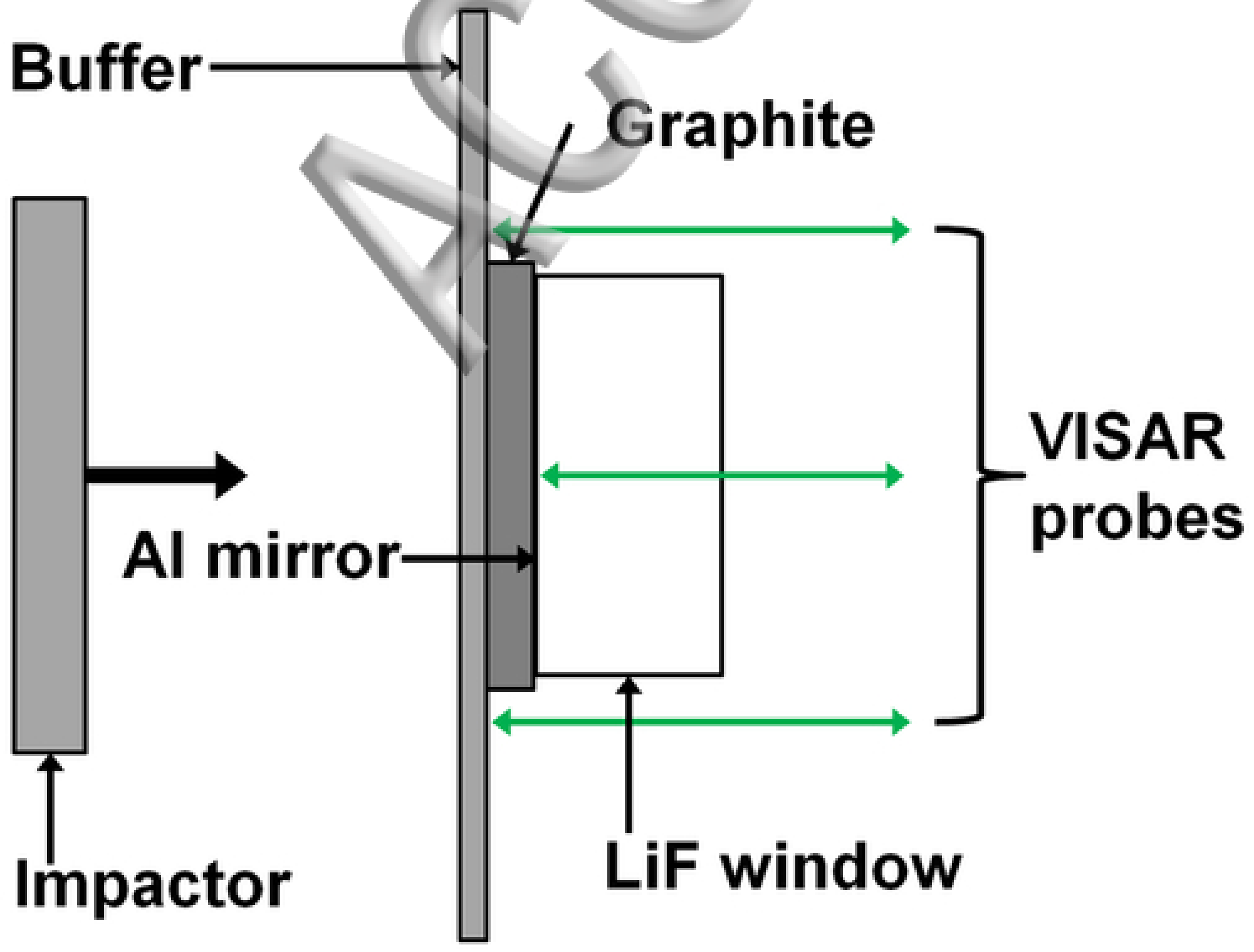
Buffer
Graphite
VISAR
probes
Al mirror
Impactor
LiF window

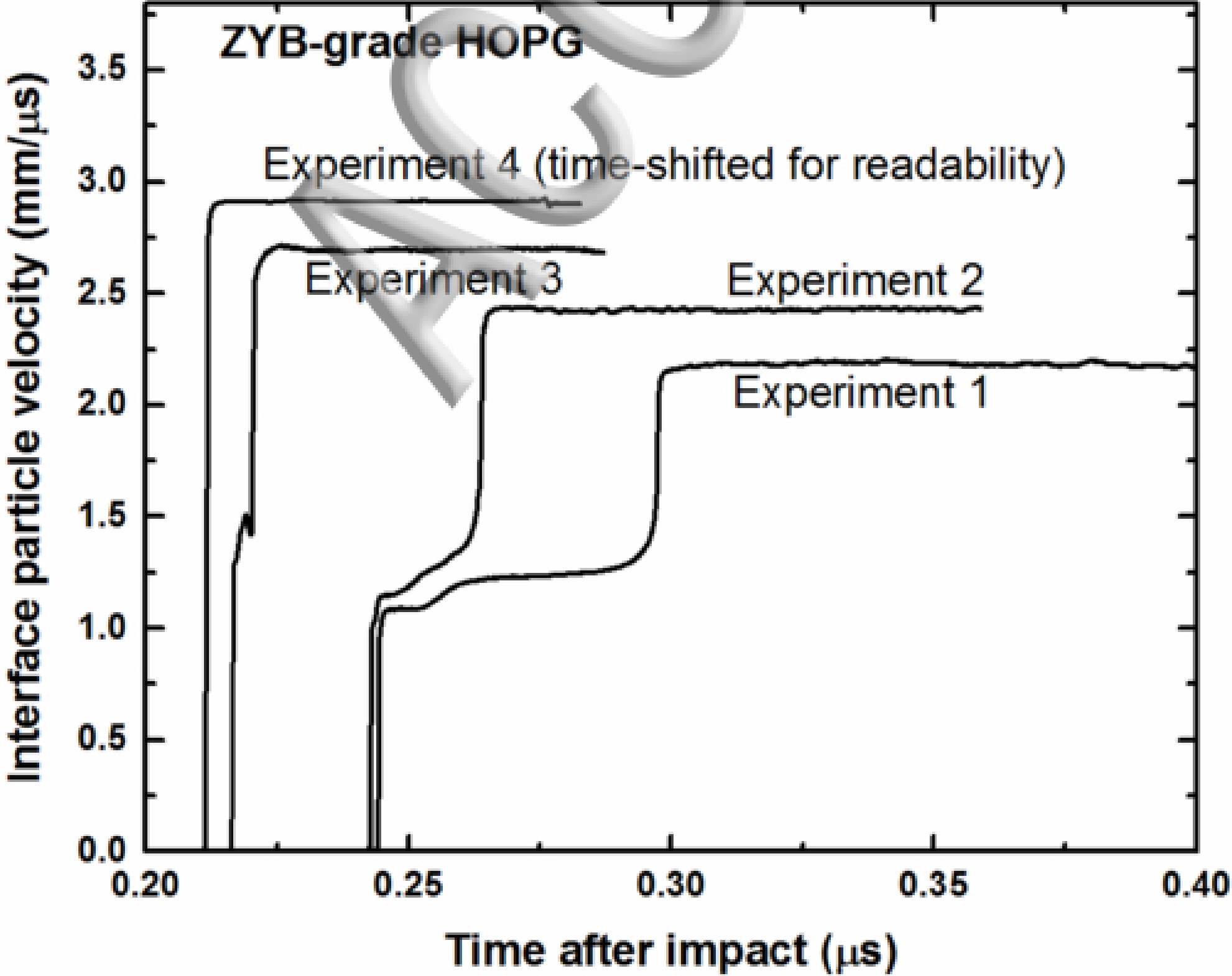
ZYB-grade HOPG
Experiment 4 (time-shifted for readability)
Experiment 3
Experiment 2
Experiment 1
Interface particle velocity (mm/μs)
Time after impact (μs)
0.0
0.5
1.0
1.5
2.0
2.5
3.0
3.5
0.20
0.25
0.30
0.35
0.40

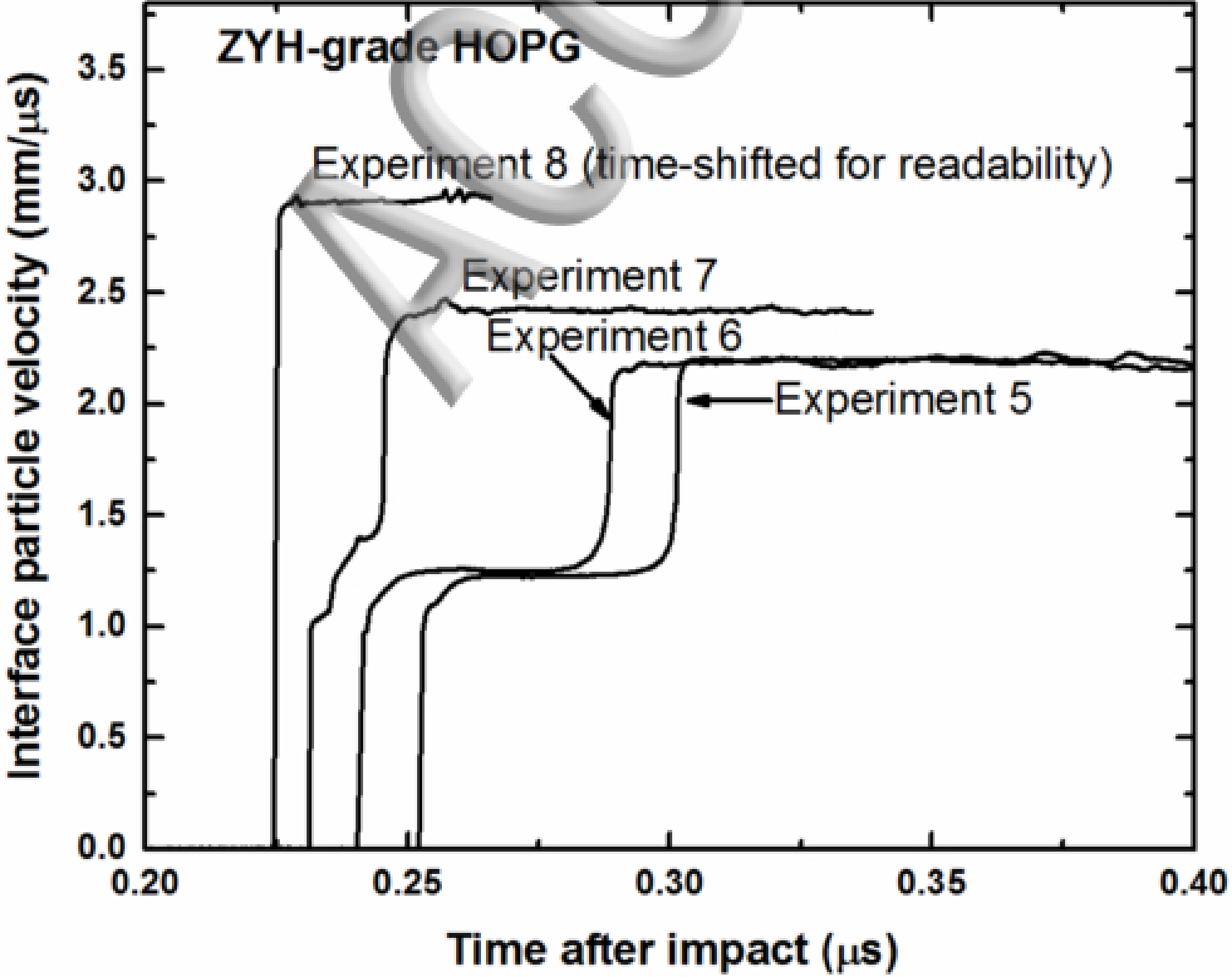
ZYH-grade HOPG
Experiment 8 (time-shifted for readability)
Experiment 7
Experiment 6
Experiment 5
Interface particle velocity (mm/μs)
Time after impact (μs)
0.0
0.5
1.0
1.5
2.0
2.5
3.0
3.5
0.20
0.25
0.30
0.35
0.40

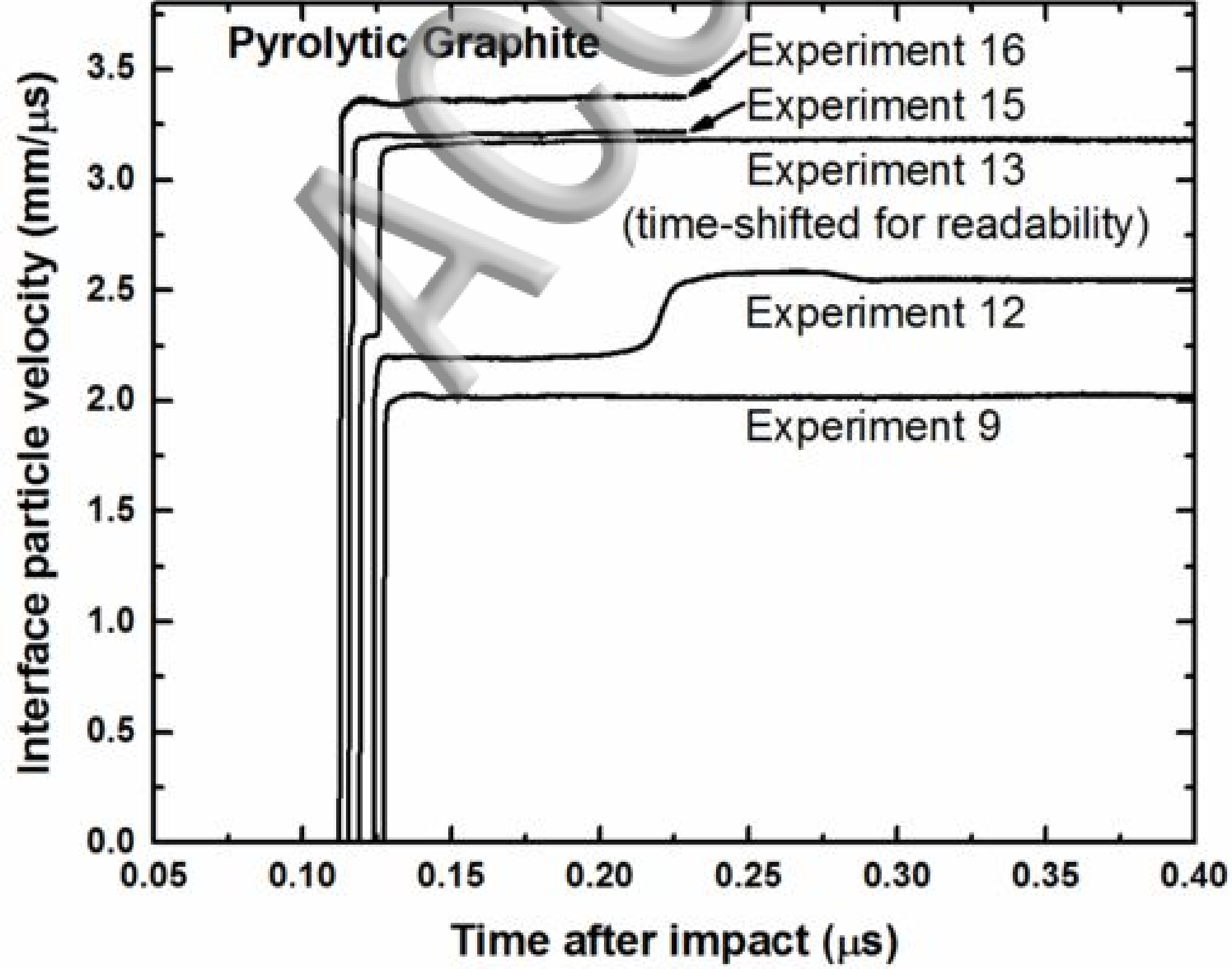
Pyrolytic Graphite
Experiment 16
Experiment 15
Experiment 13
(time-shifted for readability)
Experiment 12
Experiment 9
Interface particle velocity (mm/μs)
Time after impact (μs)
0.0
0.5
1.0
1.5
2.0
2.5
3.0
3.5
0.05
0.10
0.15
0.20
0.25
0.30
0.35
0.40

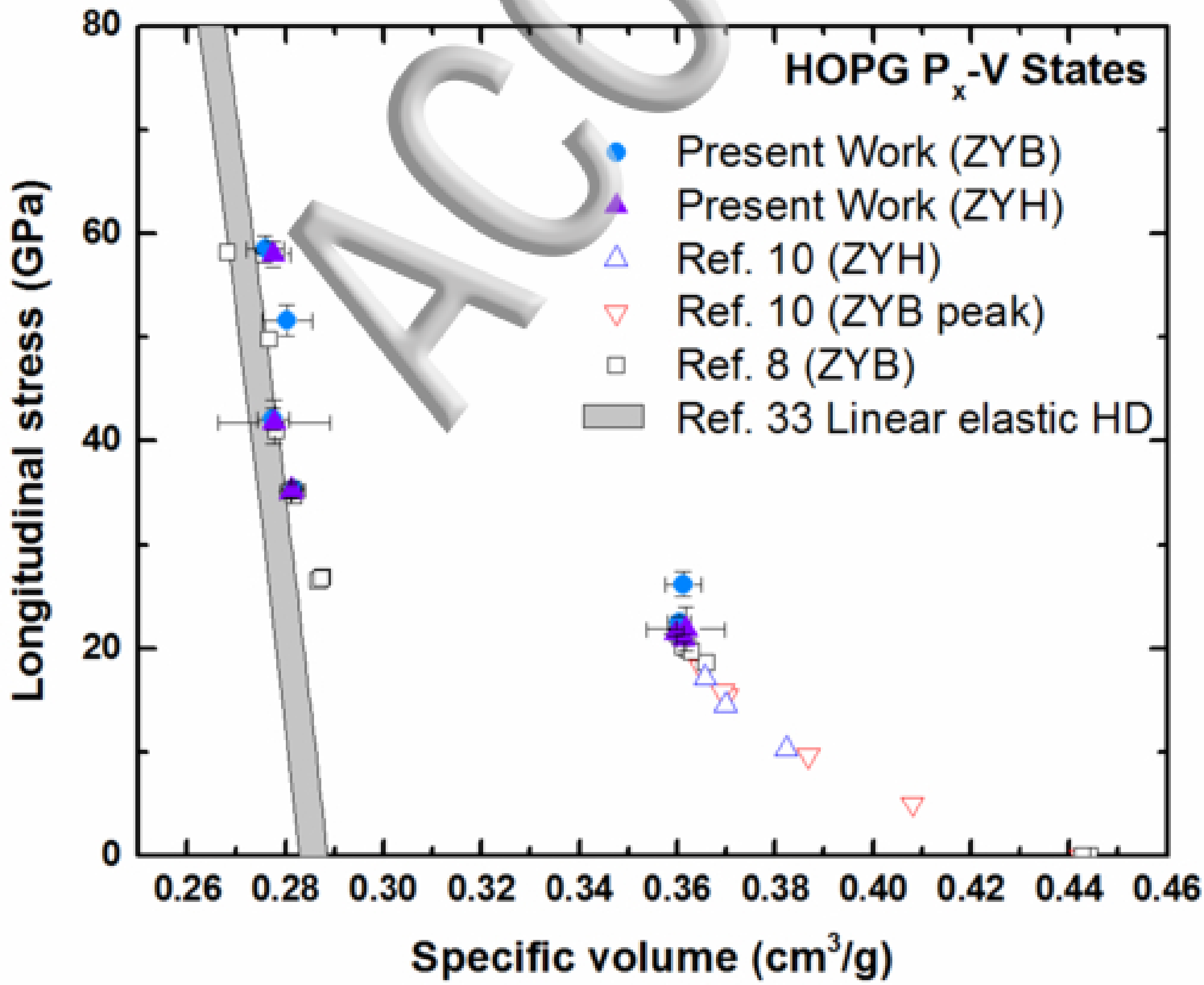
HOPG P$_x$-V States
Present Work (ZYB)
Present Work (ZYH)
Ref. 10 (ZYH)
Ref. 10 (ZYB peak)
Ref. 8 (ZYB)
Ref. 33 Linear elastic HD
Longitudinal stress (GPa)
0
20
40
60
80
0.26
0.28
0.30
0.32
0.34
0.36
0.38
0.40
0.42
0.44
0.46
Specific volume (cm^3/g)

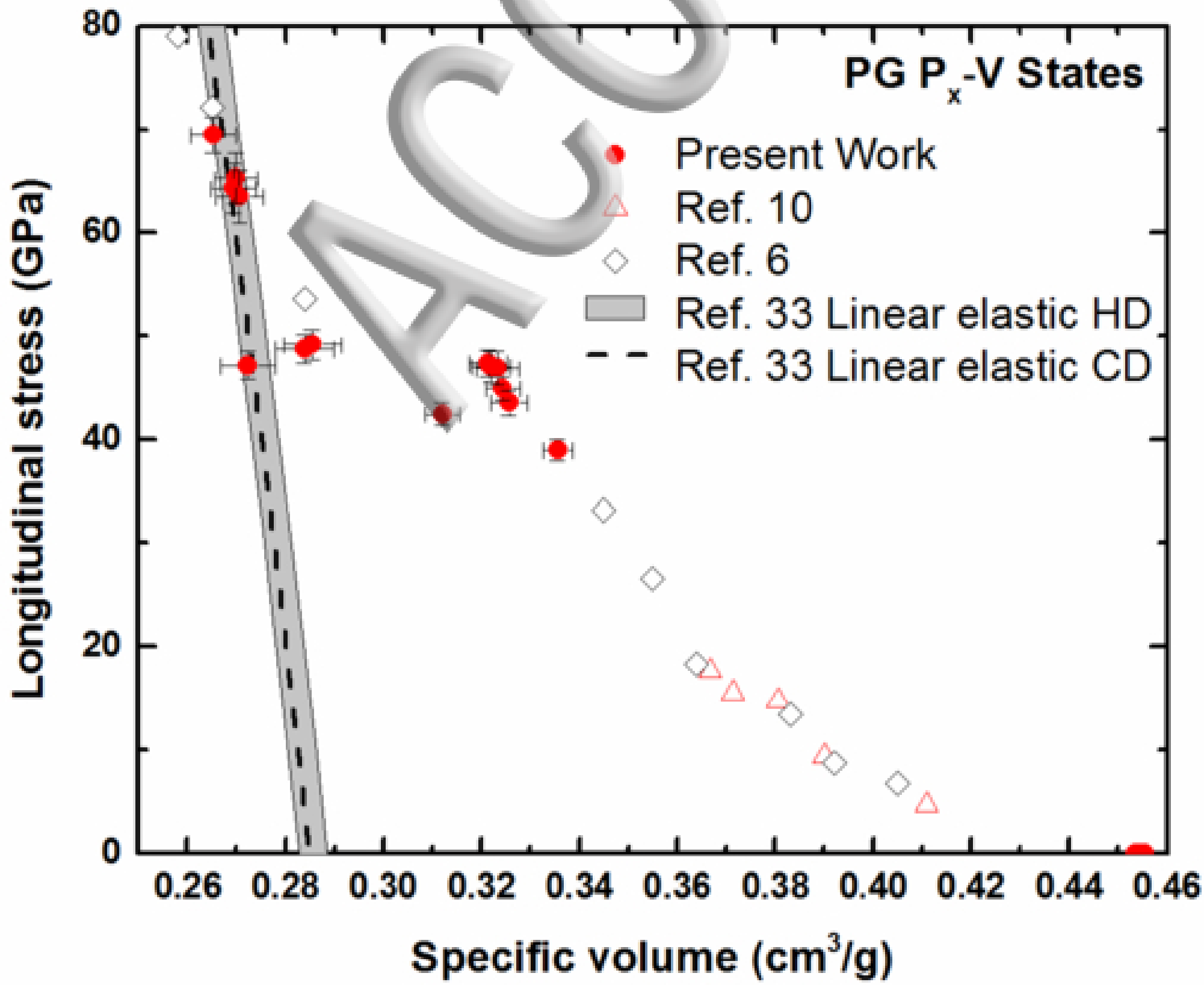
PG P_x-V States
Present Work
Ref. 10
Ref. 6
Ref. 33 Linear elastic HD
Ref. 33 Linear elastic CD
Longitudinal stress (GPa)
Specific volume (cm^3/g)
0
20
40
60
80
0.26
0.28
0.30
0.32
0.34
0.36
0.38
0.40
0.42
0.44
0.46

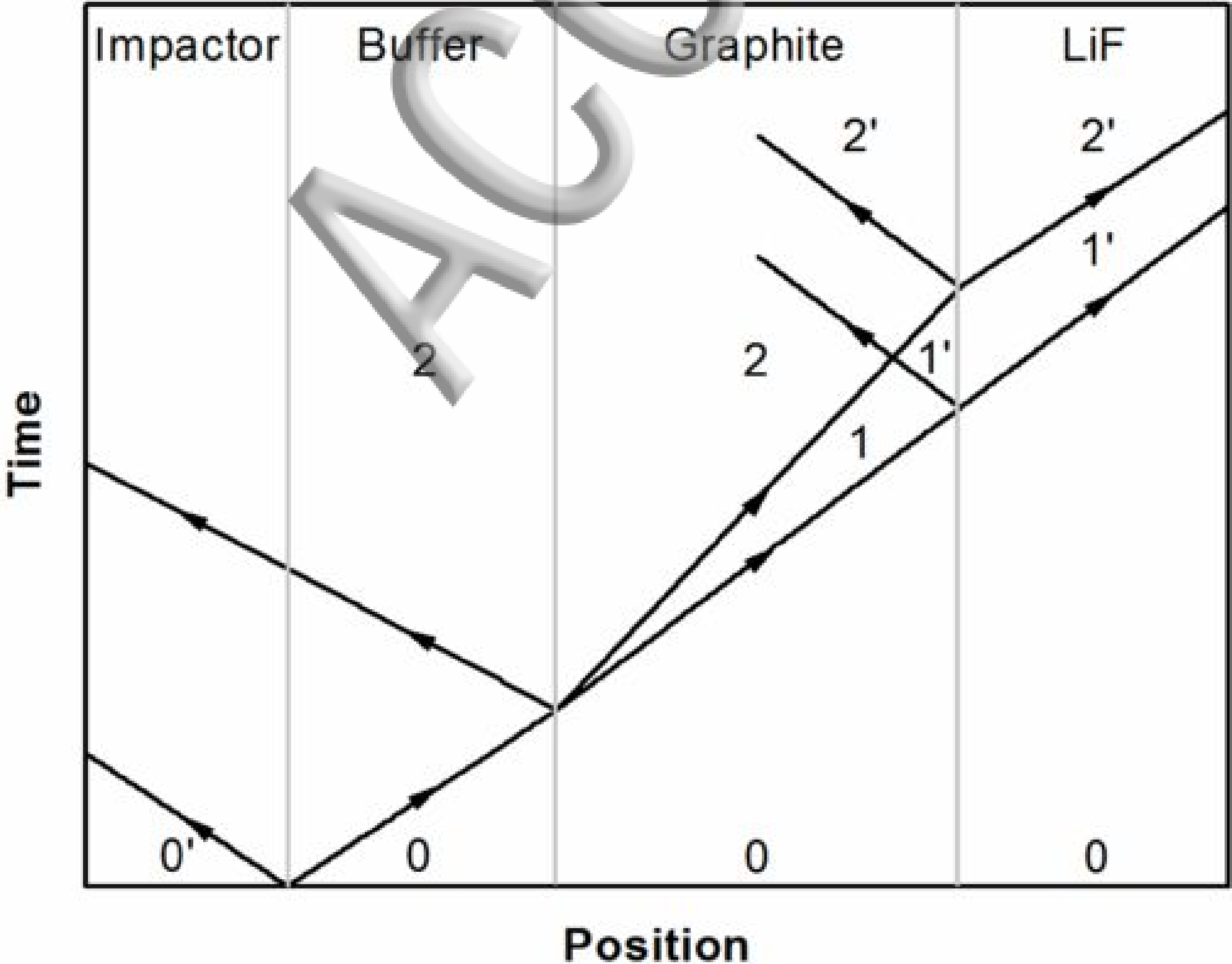
Impactor
Buffer
Graphite
LiF
2'
2'
1'
2
2
1'
1
0'
0
0
0
Time
Position

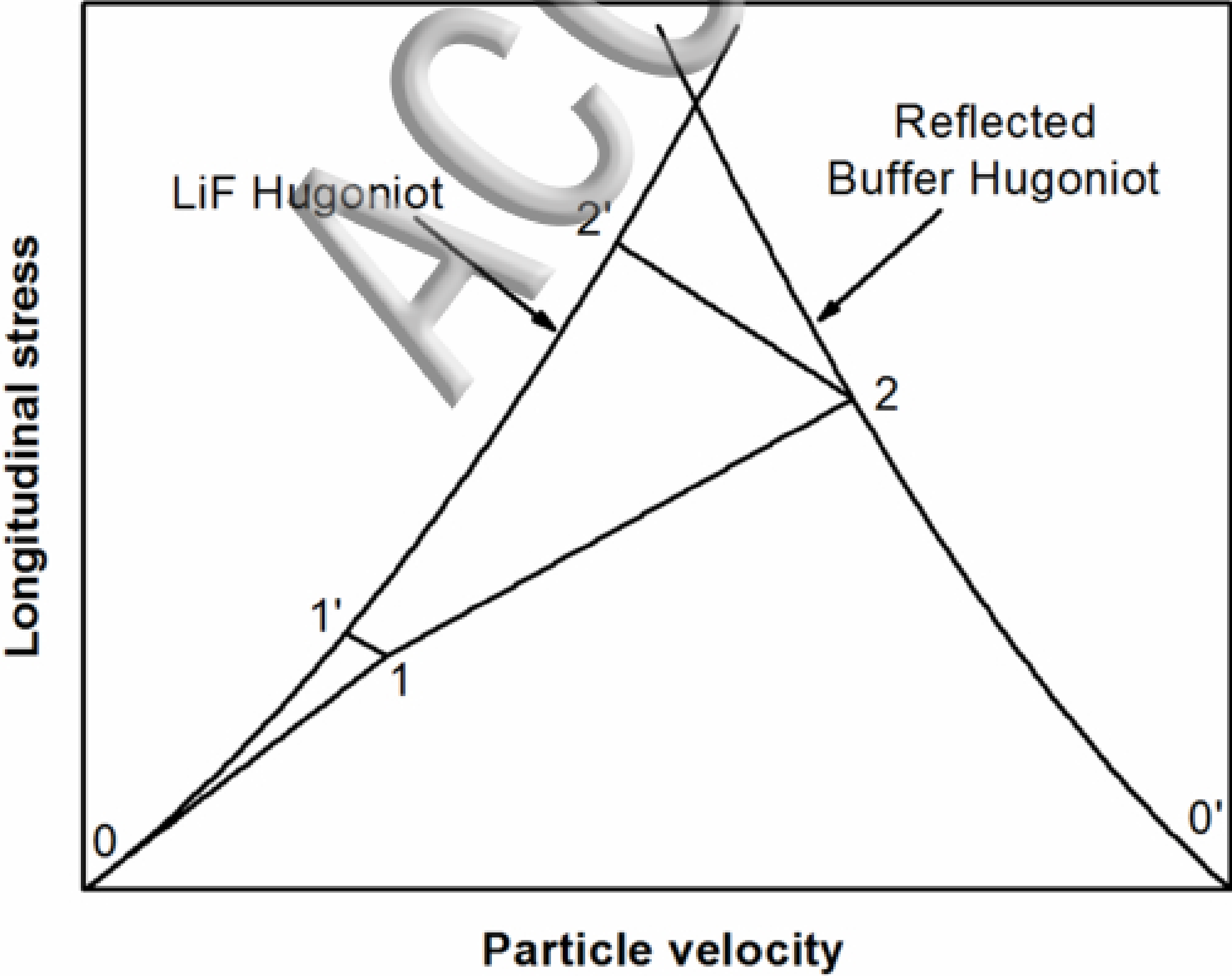
Reflected
Buffer Hugoniot
LiF Hugoniot
2'
2
1'
1
0
0'
Longitudinal stress
Particle velocity